PERGAMON International Journal of Mechanical Sciences 43 (2001) 1731–1746

International Journal of MECHANICAL SCIENCES

www.elsevier.com/locate/ijmecsci

The determination of natural frequencies of rectangular plates with mixed boundary conditions by discrete singular convolution

G.W. Wei[a,*], Y.B. Zhao[a], Y. Xiang[b]

[a] *Department of Computational Science, National University of Singapore, Singapore 117543, Singapore*
[b] *School of Engineering and Industrial Design, University of Western Sydney, Penrith South DC NSW 1797, Australia*

Received 23 March 2000; received in revised form 29 January 2001

Abstract

This paper introduces the discrete singular convolution algorithm for vibration analysis of rectangular plates with mixed boundary conditions. A unified scheme is proposed for the treatment of simply supported, clamped and transversely supported (with nonuniform elastic rotational restraint) boundary conditions. The robustness and reliability of the present approach are tested by a number of numerical experiments. All results agree well with those in the literature.

Keywords: Discrete singular convolution; Vibration analysis; Mixed boundary condition; Nonuniform boundary condition; Rectangular plate

1. Introduction

Plates with mixed boundary conditions are key components in civil and mechanical engineering and industrial design. Although theoretical analysis is valuable for providing basic understanding, in general, there is no analytical solution to the problems of vibration and buckling of rectangular plates with discontinuous boundary conditions. Therefore, numerical computation is one of the most important approaches for obtaining full solutions for theoretical analysis and engineering design. For this reason, the numerical simulation of rectangular plates with mixed

* Corresponding author. Tel.: +65-874-6589; fax: +65-774-6756.
E-mail addresses: cscweigw@nus.edu.sg (G.W. Wei), zhaoyb@czz.nus.edu.sg (Y.B. Zhao), y.xiang@uws.edu.au (Y. Xiang).

0020-7403/01/$ - see front matter
PII: S0020-7403(01)00021-2

Nomenclature

a	length of a rectangular plate
a_m	boundary extension parameters ($a_m = a_m^0$)
a_m^j	boundary extension parameters
b	width of a rectangular plate
C_m^k	DSC weight coefficients
D	flexural rigidity
$\mathbf{D}_q^n$	differential matrices
E	modulus of elasticity
f	a function
h	thickness of a rectangular plate
i	index
j	index
k	index
K	elastic rotational stiffness function
K'	nondimensional spring coefficient
l_i	dimensionless parameters in the horizontal coordinate
l_i'	dimensionless parameters in the vertical coordinate
m	index
M	DSC band width
n	the normal coordinate w.r.t the rectangular plate edge
N	maximum index of the grid points
q	the coordinates
s	the tangential coordinate w.r.t the rectangular plate edge
w	transverse displacement
W	dimensionless transverse displacement
$W_{i,j}$	grid values of the dimensionless transverse displacement
$\mathbf{W}$	a vector
x	the horizontal coordinate
X	the dimensionless horizontal coordinate
X_i	grid values of the X coordinate
y	the vertical coordinate
Y	the dimensionless vertical coordinate
Y_j	grid values of the Y coordinate

Greek letters

α	length of a support interval
$\delta_{\sigma,\Delta}$	DSC kernel
Δ	grid spacing
λ	aspect ratio
ν	Poisson's ratio
ρ	mass density
σ	a parameter in the DSC kernel
ω	circular frequency
Ω	dimensionless parameter

boundary conditions has attracted much attention in the last few decades. Numerical analysis of plates with mixed edges is not a trivial task. In particular, the problem is difficult when the discontinuous boundary conditions induce singularities in the stress distribution. A variety of numerical methods have been developed for the solution of this problem. Ota and Hamada [1] computed the fundamental frequency of a simply supported rectangular plate partially clamped on the edge by using a distributed moment function along the mixed edge. Keer and Stahl [2] formulated Fredholm integral equations of the second kind to study the same problem. They analyzed the dependence of the fundamental frequency on the clamped portion. Similar approaches were explored by many other researchers [3,4]. Narita [5] developed a series expansion algorithm to solve the problem and attained the frequency parameters for a wide range of mixed-edge rectangular plates. The reliability and robustness of the methods of finite strips, strip elements, spline elements and finite elements were intensively investigated for their use in the analysis of plates with mixed boundary conditions [6–11]. Galerkin approaches were studied by Chia [12]. Recently, the use of the (generalized) differential quadrature method for plate analysis was examined by a number of researchers [13–16]. The global Rayleigh–Ritz variational methods had a long history for their successful applications to plate vibration analysis [17–21]. The existence of so many different approaches and so much on-going effort for the analysis of plates with mixed boundary conditions indicate the practical importance and the difficulty of the problem.

All the above-mentioned methods were successful for plate analysis with discontinuous boundary conditions in one way or another. It is very difficult to have a detailed analysis of the advantages and disadvantages of all these computational approaches. However, each of these methods can be classified as either a global method (Ritz method, differential quadrature method) or a local method (finite element method, finite difference method, finite strip method). In general, global methods are highly localized in their spectral representations, but are unlocalized in the coordinate representation. By contrast, local methods have high spatial localization, but are delocalized in their spectral representations. Moreover, the use of global methods is usually restricted to structured grids, whereas, local methods can be implemented to block-structured grids and even unstructured grids. Furthermore, global methods are much more accurate than local methods, while the major advantage of local methods is the flexibility for handling complex geometries and boundary conditions. In ordinary applications of plate analysis and structural engineering, it is relatively safe and efficient to use either a global method or a local one. However, when the problem under study involves singularities, for instance, a rapid increase in stress concentration, neither the global methods nor the local methods can be applied without numerical instability and convergence problems. The global methods lose their accuracy near the singularities due to local high frequency components which require extremely high order approximations. The local methods have to be implemented in an adaptive manner, which greatly limits their accuracy and requires extremely small spatial mesh sizes. In many situations, the rate of convergence of a numerical method simply cannot match the divergent rate of the problem under study near a singularity. It is desirable to have a method that has both spectral and spatial localization, and is thus locally smooth and asymptotically decaying in both spectral and coordinate spaces. Most importantly, such a method has the global methods' accuracy and the local methods' flexibility for handling singularity problems in analysis of mechanical behavior of structures.

Recently, the discrete singular convolution (DSC) algorithm [22] was proposed as a potential approach for the computer realization of singular convolutions of Hilbert type, Abel type and delta type. These convolutions have wide ranges of practical applications such as spectral properties of time correlation functions, electrodynamics, tomography, linear response theory, processing of analytic signal, surface interpolation and solving partial differential equations. Mathematical foundation of the DSC algorithm is the theory of distributions [23]. In particular, numerical solutions to differential equations are formulated via the singular kernels of the delta type. By appropriately selecting the parameters of a DSC kernel, the DSC approach exhibits the global methods' accuracy for integration and the local methods' flexibility for handling complex geometries and boundary conditions. The DSC algorithm has found its success in solving the Fokker–Planck equation [22], the Schrödinger equation [24], Maxwell's equations [25], the Navier–Stokes equation [26,27] and for image restoration from noise [28]. Most recently, the DSC algorithm was used to resolve some numerically challenging problems. It was utilized to integrate the sine-Gordon equation with the initial values close to and on a homoclinic manifold singularity [29] for which conventional local methods encountered great difficulties and resulted in numerically induced spatial and temporal chaos [30]. Another complex example that was resolved by using the DSC algorithm is the integration of the Cahn–Hilliard equation in a circular domain, which is challenging because of the fourth order artificial singularity at the origin and the complex phase space geometry [31].

The further developments, which are relevant to the present work, are the use of the DSC algorithm for analysis of mechanical behavior of structures [32,26,33,34]. Previous works have shown that the DSC approach provided more than 10 significant figures accuracy for the first 100 eigenmodes of a rectangular plate vibration with simply supported boundary conditions [32,26]. The vibration of circular plates was also analyzed with clamped boundary conditions [26]. Extremely accurate DSC results were obtained for beam bending, vibration and buckling [33,34]. However, the boundary conditions and the corresponding treatment in these works are relatively simple and uniform. The objective of the present study is to extend the previous implementation of the DSC algorithm for rectangular plate analysis to mixed boundary conditions.

This paper is organized as follows. In Section 2, we describe the DSC algorithm for the treatment of vibration of plates. A unified scheme is developed to implement the DSC algorithm for the analysis of plates with arbitrarily mixed boundary conditions. Numerical experiments and convergence tests are presented in Section 3. This paper ends with a conclusion.

2. Method of analysis

In this section, the DSC algorithm for treating various boundary conditions is discussed in the context of plate vibration analysis, while the approach can be used for many other applications. We limit our attention to the vibration of rectangular (classic) Kirchhoff plates with simply supported, clamped and transversely supported edges. Consider a rectangular plate which has a length a, width b, thickness h, mass density ρ, modulus of elasticity E, and Poisson's ratio v (see Fig. 1).

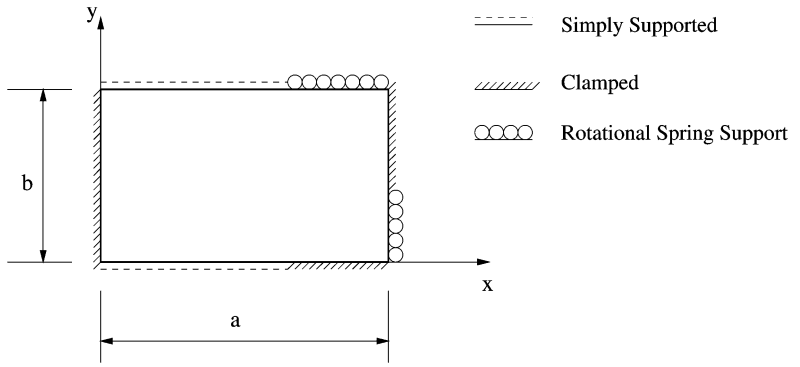

Fig. 1. Geometry and coordinate system of a rectangular plate with mixed edge supports.

The governing differential equation for the plate is given by [35]

$$\frac{\partial^4 w}{\partial x^4} + 2\frac{\partial^4 w}{\partial x^2 \partial y^2} + \frac{\partial^4 w}{\partial y^4} = \frac{\rho h \omega^2}{D} w, \tag{1}$$

where $w(x, y)$ is the transverse displacement of the midsurface of the plate, $D = Eh^3/[12(1-\nu^2)]$ the flexural rigidity, and ω the circular frequency. We consider one of the following three types of support conditions for each plate edge:

For simply supported edge (S):

$$w = 0, \quad -D\left(\frac{\partial^2 w}{\partial n^2} + \nu\frac{\partial^2 w}{\partial s^2}\right) = 0. \tag{2}$$

For clamped edge (C):

$$w = 0, \quad \frac{\partial w}{\partial n} = 0. \tag{3}$$

For transversely supported edge with nonuniform elastic rotational restraint (E):

$$w = 0, \quad -D\left(\frac{\partial^2 w}{\partial n^2} + \nu\frac{\partial^2 w}{\partial s^2}\right) = K(s)\frac{\partial w}{\partial n}, \tag{4}$$

where $K(s)$ is the varying elastic rotational stiffness of the plate elastic edge and n and s denote, respectively, the normal and tangential coordinates with respect to the rectangular plate edge.

For generality and simplicity, the following dimensionless parameters are introduced:

$$X = \frac{x}{a}, \quad Y = \frac{y}{b}, \quad W = \frac{w}{a}, \quad \lambda = \frac{a}{b}, \quad \Omega = \omega a^2\sqrt{\frac{\rho h}{D}}. \tag{5}$$

Accordingly, we obtain the dimensionless governing equation for the vibration analysis of a rectangular plate as

$$\frac{\partial^4 W}{\partial X^4} + 2\lambda^2\frac{\partial^4 W}{\partial X^2 \partial Y^2} + \lambda^4\frac{\partial^4 W}{\partial Y^4} = \Omega^2 W. \tag{6}$$

Consider a uniform grid having

$$0 = X_0 < X_1 < \cdots < X_N = 1$$

and

$$0 = Y_0 < Y_1 < \cdots < Y_N = 1.$$

To formulate the eigenvalue problem, we introduce a column vector $\mathbf{W}$ as

$$\mathbf{W} = (W_{0,0}, \ldots, W_{0,N}, W_{1,0}, \ldots, W_{N,N})^{\mathrm{T}}, \tag{7}$$

with $(N+1)^2$ entries $W_{i,j} = W(X_i, Y_j)$, $(i, j = 0, 1, \ldots, N)$.

Let us define the $(N+1) \times (N+1)$ differential matrices $\mathbf{D}_q^n$ $(q = X, Y;\ n = 1, 2, \ldots)$, with their elements given by

$$[\mathbf{D}_q^n]_{i,j} = \delta_{\sigma,\Delta}^{(n)}(q_i - q_j) \quad (i, j = 0, \ldots, N), \tag{8}$$

where $\delta_{\sigma,\Delta}(q_i - q_j)$ is a DSC kernel of the delta type [22]. Here Δ is the grid spacing and σ determines the effective computational bandwidth. Many DSC kernels were constructed in the original work. Here, we choose a simple example, the regularized Shannon's delta kernel

$$\delta_{\sigma,\Delta}(q - q_j) = \frac{\sin[(\pi/\Delta)(q - q_j)]}{(\pi/\Delta)(q - q_j)} \mathrm{e}^{-((q-q_j)^2/2\sigma^2)} \tag{9}$$

to illustrate the algorithm and its application. Other DSC kernels were discussed in the original work [22]. The performance of a few DSC kernels for fluid dynamic computations and structural analysis was compared in Ref. [32]. The differentiation in Eq. (8) can be *analytically* carried out as

$$\delta_{\sigma,\Delta}^{(n)}(q_i - q_j) = \left[\left(\frac{\mathrm{d}}{\mathrm{d}q}\right)^n \delta_{\sigma,\Delta}(q - q_j)\right]_{q=q_i} = C_m^n, \tag{10}$$

where, for a uniform grid spacing, $m = (q_i - q_j)/\Delta$. Here the matrix is banded to $i - j = m = -M, \ldots, 0, \ldots, M$. Therefore, the system of linear algebraic equations for the governing PDE (6) is given by

$$(\mathbf{D}_X^4 \otimes \mathbf{I} + 2\lambda^2 \mathbf{D}_X^2 \otimes \mathbf{D}_Y^2 + \lambda^4 \mathbf{I} \otimes \mathbf{D}_Y^4)\mathbf{W} = \Omega^2 \mathbf{W}, \tag{11}$$

where $\mathbf{I}$ is the $(N+1)^2$ unit matrix and $\otimes$ denotes the tensorial product. Eigenvalues can be evaluated from Eq. (11) by using a standard solver. However, appropriate boundary conditions are to be implemented before calculating eigenvalues. This is described below.

We first note that boundary condition $W = 0$ is easily specified at the edge. To implement other boundary conditions, we assume, for a function f, the following relation between the inner nodes and the outer nodes on the left boundary:

$$f(X_{-m}) - f(X_0) = \left(\sum_{j=0}^{J} a_m^j X_m^j\right)[(f(X_m) - f(X_0)], \tag{12}$$

where coefficients a_m^j $(m = 1, \ldots, M,\ j = 0, 1, \ldots, J)$ are to be determined by the boundary conditions. For the three types of boundary conditions described earlier, we only need to consider

the zeroth order term in the power of X^j. Therefore we set $a_m^0 \equiv a_m$ and, after rearrangement, obtain

$$f(X_{-m}) = a_m f(X_m) + (1 - a_m) f(X_0), \quad m = 1, 2, \ldots, M. \tag{13}$$

According to Eq. (10), the first and the second derivatives of f on the boundary are approximated by

$$f'(X_0) = \sum_{m=-M}^{M} C_m^1 f(X_m) \tag{14}$$

$$= \left[C_0^1 - \sum_{m=1}^{M} (1 - a_m) C_m^1 \right] f(X_0) + \sum_{m=1}^{M} (1 - a_m) C_m^1 f(X_m) \tag{15}$$

and

$$f''(X_0) = \sum_{m=-M}^{M} C_m^2 f(X_m)$$

$$= \left[C_0^2 + \sum_{m=1}^{M} (1 - a_m) C_m^2 \right] f(X_0) + \sum_{m=1}^{M} (1 + a_m) C_m^2 f(x_m),$$

respectively. Here, the symmetries of the DSC coefficients have been used.

For simply supported edges, the boundary conditions reduce to

$$f(X_0) = 0, \quad f''(X_0) = 0. \tag{16}$$

These are satisfied by choosing $a_m = -1$, $m = 1, 2, \ldots, M$. This is the so called *anti-symmetric extension* [22].

For clamped edges, the boundary conditions require

$$f(X_0) = 0, \quad f'(X_0) = 0. \tag{17}$$

These are satisfied by $a_m = 1$, $m = 1, 2, \ldots, M$. This is the *symmetric extension* [22].

For a transversely supported edge, the boundary conditions are

$$f(X_0) = 0, \quad f''(X_0) + K f'(X_0) = 0. \tag{18}$$

Hence, the equation is given by

$$\sum_{m=1}^{M} (1 + a_m) C_m^2 f(X_m) + K \sum_{m=1}^{M} (1 - a_m) C_m^1 f(X_m) = 0. \tag{19}$$

Further simplification of the above equation gives

$$\sum_{m=1}^{M} [(1 + a_m) C_m^2 + K(1 - a_m) C_m^1] f(X_m) = 0. \tag{20}$$

One way to satisfy Eq. (20) is to choose

$$a_m = \frac{K C_m^1 + C_m^2}{K C_m^1 - C_m^2}, \quad m = 1, 2, \ldots, M. \tag{21}$$

Expressions for the right, top and bottom boundaries can be derived in a similar way.

For the continuous nonuniform (elastic) boundary conditions, the rotational spring coefficients $K_1(Y)$, $K_2(Y)$, $K_3(X)$ and $K_4(X)$ are taken as

$$K_1(Y) = K_2(Y) = K' \frac{(Y - l_1)(l_2 - Y)}{(l_2 - l_1)} \quad (0 \leqslant l_1 < l_2 \leqslant 1), \tag{22}$$

$$K_3(X) = K_4(X) = K' \frac{(X - l_1')(l_2' - X)}{(l_2' - l_1')\lambda} \quad (0 \leqslant l_1' < l_2' \leqslant 1), \tag{23}$$

where K' is the nondimensional spring coefficient, $K' = K_0 a^3/D$, and $l_1(l_1'), l_2(l_2')$ are the nondimensional starting and ending points of elastic boundary, respectively. Obviously, the implementation of the rotational spring coefficients leads to a minor modification of the matrix in Eq. (11).

3. Results and discussion

Numerical solutions for the vibration of rectangular plates with mixed boundary conditions are presented to illustrate the versatility, accuracy and reliability of the DSC algorithm. Convergence tests and comparison studies are carried out to ascertain the validity of the proposed method for the undertakings. Two sets of DSC parameters are used, i.e., $\sigma = 2.8\Delta$ when $M = 25$ (used in convergence studies), and $\sigma = 3.2\Delta$ when $M = 32$ (used in all other calculations). Qian and Wei [36] have shown that there is a wide range of σ values that provide accurate and reliable results. The present choices fall in the "reliable range" of σ values.

3.1. Convergence study

We consider five different cases (see Table 1) to investigate the convergence of the DSC algorithm. These include the mixing between simply supported and clamped boundary conditions (Cases 1 and 2), the mixing between transversely supported and clamped edges (Case 3), and the mixing between transversely supported and simply supported edges (Cases 4 and 5).

In all convergence tests, we examine the consistency of the first five eigenvalues with respect to the variation of grid size N. In Case 1, a simply supported plate partially clamped at one edge, we observe a very good overall convergence over a number of grid sizes. In fact, the third eigenvalue converges slightly slower compared to others. Therefore, the third eigenmode must have a node distribution which is very sensitive to the discontinuity at the mixing point of two boundary conditions. Case 2 has a partially simply supported and partially clamped configuration. Such a case is more difficult to converge due to the stress concentration induced by the discontinuous boundary conditions. However, the DSC performs quite well for this case. Very good convergence is observed for modes 3 and 4.

In Case 3, the mixing is between clamped and transversely supported edges. Uniform rotational spring support along the boundary is considered in this case and the nondimensional spring coefficients are chosen as $K = 100$. For this case, we have observed very good convergence. In the last two calculations, we have also chosen the nondimensional spring coefficient $K' = 100$. It is observed that an arbitrary combination between simply supported and transversely supported edges produces little problem for the present computations. It is noted that the Rayleigh–Ritz

Table 1
Convergence study of the frequency parameters

Boundary conditions	Mesh size	Ω_1	Ω_2	Ω_3	Ω_4	Ω_5
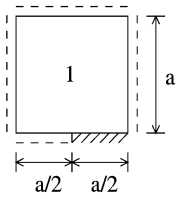	$N=26$	22.40	49.87	55.50	82.26	99.66
	$N=28$	22.41	49.87	55.51	82.26	99.66
	$N=30$	22.42	49.88	55.52	82.26	99.66
	$N=32$	22.42	49.88	55.53	82.26	99.66
	$N=34$	22.42	49.88	55.54	82.26	99.67
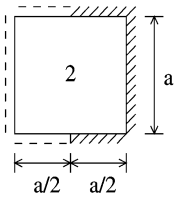	$N=26$	27.75	60.33	61.00	94.55	111.80
	$N=28$	27.77	60.37	61.00	94.54	111.85
	$N=30$	27.78	60.40	61.00	94.54	111.88
	$N=32$	27.80	60.43	61.00	94.54	111.92
	$N=34$	27.81	60.45	61.00	94.54	111.94
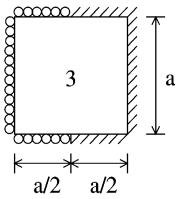	$N=26$	35.38	72.20	72.21	106.56	129.57
	$N=28$	35.38	72.19	72.20	106.54	129.55
	$N=30$	35.38	72.19	72.20	106.53	129.53
	$N=32$	35.38	72.18	72.20	106.52	129.52
	$N=34$	35.38	72.18	72.20	106.51	129.51
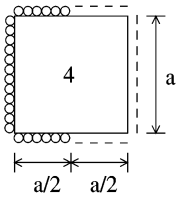	$N=26$	24.36	54.21	57.00	86.87	103.89
	$N=28$	24.35	54.20	56.98	86.86	103.88
	$N=30$	24.35	54.20	56.98	86.85	103.87
	$N=32$	24.35	54.19	56.98	86.84	103.86
	$N=34$	24.35	54.19	56.98	86.83	103.85
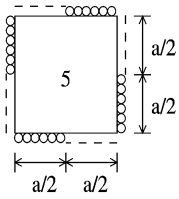	$N=26$	24.55	54.97	54.97	85.15	104.92
	$N=28$	24.55	54.96	54.96	85.13	104.90
	$N=30$	24.54	54.96	54.96	85.13	104.88
	$N=32$	24.54	54.95	54.95	85.12	104.86
	$N=34$	24.54	54.95	54.95	85.11	104.85

method generates upper bound solutions, whereas, the present approach generates results from the differential equation and its solution cannot be determined as being upper bound or lower bound. However, for a reasonable grid size, the DSC solution becomes grid independent and converges to the exact solution [26].

Table 2
Natural frequencies of simply supported but partially clamped square plates

Boundary conditions		Ω_1	Ω_2	Ω_3	Ω_4	Ω_5
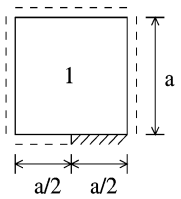	Nowacki [38], Ota and Hamada [1]	22.4	—	—	—	—
	Cheung [7]	22.5	—	—	—	—
	Keer and Stahl [2]	22.49	—	—	—	—
	Rao et al. [10]	22.96	—	—	—	—
	Narita [5]	22.63	50.04	55.95	82.34	99.71
	Gorman [39]	22.48	—	—	—	—
	Fan and Cheung [6]	22.73	50.15	56.23	—	—
	Mizusawa et al. [11]	22.71	50.10	56.13	82.37	99.73
	Liew et al. [37]	22.40	—	—	—	—
	Laura et al. [14]	21.99	—	—	—	—
	Shu and Wang [16]	22.42	49.93	55.51	82.32	99.64
	DSC	22.42	49.88	55.54	82.26	99.67
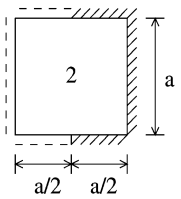	Piskunov [40]	26.3	—	—	—	—
	Cheung [7]	28.1	—	—	—	—
	Fan and Cheung [6]	28.65	61.06	62.48	—	—
	Mizusawa et al. [11]	28.58	61.01	62.23	94.53	113.40
	Shu and Wang [16]	28.28	61.01	61.56	94.29	113.92
	DSC	27.81	60.45	61.00	94.54	111.94
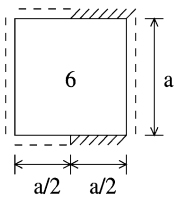	Ota and Hamada [1]	25.5	—	—	—	—
	Cheung [7]	25.9	—	—	—	—
	Fan and Cheung [6]	26.37	52.23	61.78	—	—
	Laura et al. [14]	25.41	—	—	—	—
	DSC	25.59	52.10	59.80	88.14	100.54

While Cases 1 and 2 are standard testing problems in the literature, we noted that Cases 3, 4 and 5 have not been previously reported. In the next section, comparison is made between the present DSC results and those in the literature.

3.2. Plates with simply supported but partially clamped edges

Unlike the simply supported case which admits an analytical solution, plates with mixed boundary conditions have no analytical solution available yet. To further validate the present algorithm, we compare the DSC results with those available in the literature. We first examine the natural frequencies of simply supported but partially clamped square plates. This problem has been investigated by a number of researchers for testing their computational methods.

In Table 2, the results obtained by using the DSC approach are listed for the first five eigenvalues. For Case 1, the DSC eigenvalues agree with previous results. In particular, we have an excellent agreement with those of Shu and Wang [16] obtained by using their generalized

Table 3
Natural frequencies of simply supported but partially clamped square plates centered in the middle with different width ratios

	Ratio		Ω_1	Ω_2	Ω_3	Ω_4	Ω_5
	$\frac{1}{4}$	Cheung [7]	26.46	50.83	61.11	—	—
		Fan and Cheung [6]	27.27	51.63	64.72	—	—
		DSC	26.38	50.64	62.35	82.26	98.85
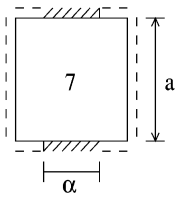	$\frac{1}{3}$	Kurata and Okamura [41]	27.31				
		Keer and Stahl [2]	27.30				
		Rao et al. [10]	27.85				
		Narita [5]	28.10	52.85	66.86	—	—
		Cheung [7]	27.63	52.39	66.24	—	—
		Fan and Cheung [6]	27.83	52.41	66.25	—	—
		DSC	27.23	51.51	64.49	84.65	99.16
	$\frac{1}{2}$	Ota et al. [1]	28.3	—	—	—	—
		Keer and Stahl [2]	28.37	—	—	—	—
		Rao et al. [10]	28.62	—	—	—	—
		Narita [5]	28.44	53.49	67.85	—	—
		Cheung [7]	28.94	54.26	68.07	—	—
		Fan and Cheung [6]	28.65	54.00	68.58	—	—
		DSC	28.36	53.29	67.60	89.87	100.39
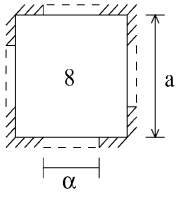	$\frac{1}{2}$	Liew et al. [37]	24.72	56.97	—	96.37	100.6
		Narita [5]	26.18	58.70	58.70	98.58	102.0
		DSC	26.66	56.90	62.30	96.33	105.26

differential quadrature method. Case 2 is a half simply supported and half clamped plate. We have observed that the DSC eigenvalues are slightly smaller than those of Shu and Wang [16], and of Mizusawa et al. [9] except for the 4th mode. The last example listed in Table 2 is Case 6, which is a simply supported plate partially clamped at the end of two opposite edges. This case was studied by Fan and Cheung [6] by using the finite strip method, and others [1,7,14]. The DSC results are consistent with those obtained by other methods.

In the rest of this subsection, we examine the DSC approach for variable ratio of the clamped edge in mainly simply supported plates (see Table 3).

The ratio of the clamped edge in Case 7 varies from $\frac{1}{4}$, $\frac{1}{3}$ to $\frac{1}{2}$. This case was studied by Ota et al. [1], Narita [5], Cheung [7], Fan and Cheung [6], and Keer and Stahl [2]. We have listed the first five eigenvalues obtained by the DSC approach. It is found that the DSC results are in excellent agreement with those of other authors. Case 8 is a simply supported rectangular plate clamped at the four corners. Even for the first eigenvalue, a large discrepancy exists in the

Table 4
Frequency parameters for plate having mixed and nonuniform boundary conditions

	λ	K'		Ω_1	Ω_2	Ω_3	Ω_4	Ω_5
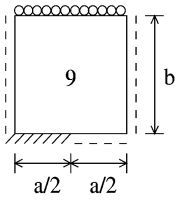	0.5	0	Shu and Wang [16]	12.773	21.014	34.115	42.107	49.643
			DSC	12.767	20.994	34.072	42.104	49.597
		0.1	Shu and Wang [16]	12.776	21.020	34.123	42.108	49.646
			DSC	12.770	21.001	34.081	42.104	49.600
		1	Shu and Wang [16]	12.799	21.072	34.190	42.113	49.669
			DSC	12.796	21.058	34.158	42.111	49.628
		10	Shu and Wang [16]	12.966	21.473	34.747	42.160	49.860
			DSC	12.976	21.496	34.773	42.162	49.847
		100	Shu and Wang [16]	13.336	22.517	36.456	42.328	50.508
			DSC	13.339	22.531	36.485	42.335	50.519
		10^6	Shu and Wang [16]	13.490	23.015	37.410	42.455	50.983
			DSC	13.483	22.992	37.361	42.453	50.958
	1.0	0	Shu and Wang [16]	22.420	49.932	55.494	82.308	99.641
			DSC	22.424	49.881	55.535	82.262	99.665
		0.1	Shu and Wang [16]	22.433	49.937	55.512	82.318	99.643
			DSC	22.438	49.888	55.553	82.273	99.667
		1	Shu and Wang [16]	22.544	49.985	55.656	82.406	99.660
			DSC	22.562	49.942	55.714	82.373	99.687
		10	Shu and Wang [16]	23.426	50.387	56.904	83.194	99.816
			DSC	23.520	50.385	57.086	83.250	99.861
		100	Shu and Wang [16]	25.891	51.818	61.638	86.742	100.579
			DSC	25.977	51.844	61.884	86.921	100.659
		10^6	Shu and Wang [16]	27.191	52.950	65.065	90.288	101.508
			DSC	27.195	52.908	65.094	90.260	101.539
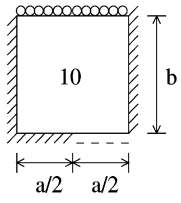	0.5	0	Shu and Wang [16]	24.065	29.895	40.898	57.256	63.662
			DSC	24.064	29.892	40.893	57.251	63.666
		0.1	Shu and Wang [16]	24.066	29.899	40.905	57.264	63.662
			DSC	24.066	29.897	40.901	57.261	63.667
		1	Shu and Wang [16]	24.079	29.937	40.964	57.337	63.666
			DSC	24.080	29.940	40.969	57.344	63.672
		10	Shu and Wang [16]	24.172	30.234	41.453	57.954	63.701
			DSC	24.181	30.264	41.510	58.037	63.711
		100	Shu and Wang [16]	24.383	31.014	42.950	60.106	63.834
			DSC	24.389	31.040	43.014	60.224	63.847
		10^6	Shu and Wang [16]	24.472	31.383	43.769	61.450	63.945
			DSC	24.472	31.381	43.766	61.451	63.949

literature between the results of Narita [5] obtained by using the series expansion and those of Liew et al. [37] obtained by using the Rayleigh based substructure method. The present DSC results agree well with that of Narita [5] for mode 1 and those of Liew et al. [37] for modes 2 and 4.

Table 4 (*continued*)

λ	K'		Ω_1	Ω_2	Ω_3	Ω_4	Ω_5
1.0	0	Shu and Wang [16]	30.973	59.807	70.445	96.760	110.942
		DSC	31.003	59.913	70.452	96.822	111.065
	0.1	Shu and Wang [16]	30.983	59.824	70.449	96.770	110.960
		DSC	31.014	59.931	70.456	96.832	111.086
	1	Shu and Wang [16]	31.067	59.968	70.482	96.854	111.126
		DSC	31.108	60.094	70.493	96.928	111.274
	10	Shu and Wang [16]	31.743	61.199	70.733	97.604	112.612
		DSC	31.846	61.452	70.813	97.759	112.935
	100	Shu and Wang [16]	33.674	65.566	72.035	100.879	119.253
		DSC	33.778	65.875	72.109	101.124	119.789
	10^6	Shu and Wang [16]	34.691	68.317	73.274	103.913	125.232
		DSC	34.735	68.445	73.280	103.963	125.387

Table 5
Frequency parameters for plate having mixed and nonuniform boundary conditions

	K'	Ω_1	Ω_2	Ω_3	Ω_4	Ω_5
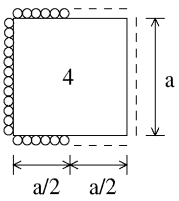	0	19.739	49.348	49.348	78.957	98.696
	0.1	19.757	49.360	49.371	78.974	98.707
	1	19.909	49.466	49.572	79.124	98.804
	10	21.081	50.383	51.260	80.474	99.671
	100	24.351	54.187	56.973	86.834	103.852
	10^6	27.806	60.446	61.000	94.535	111.939
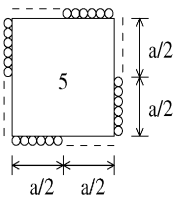	0	19.739	49.348	49.348	78.957	98.696
	0.1	19.749	49.358	49.358	78.970	98.704
	1	19.835	49.451	49.451	79.083	98.777
	10	20.617	50.300	50.300	80.114	99.483
	100	24.539	54.948	54.948	85.113	104.847
	10^6	31.474	64.254	64.254	91.936	115.824

3.3. Plates with mixed and nonuniform edges

Plates with mixed and nonuniform edges received relatively less attention in the literature. By using the global generalized differential quadrature method, Shu and Wang [16] provided some results for the Cases 9 and 10 with a range of spring coefficients varying from 0 to 10^6. The partial supports of the spring extend over one half of the plate edge length. We have carried out the same computations on these two configurations. The DSC results are compared with those of Shu and Wang in Table 4. The agreement between the two approaches are satisfactory.

Based on the confidence from the convergence study of partially transversely supported edges (Cases 4 and 5), we also enlist the spring coefficient variation study of these two cases in Table 5.

The results are presented for a variety of nondimensional spring coefficients K' of 0, 0.1, 1.0, 10, 100 and 10^6. In fact, the amplitude of the spring coefficient K' can be used to model physical condition varying from simply supported ($K'=0$) to clamped ($K' \to \infty$). In both cases computed, all five frequencies increase monotonically as the nondimensional spring coefficient increases from 0 to 10^6. This problem does not admit an analytical solution. Based on the accuracy and convergence tests conducted in the last section, it is believed that the DSC results are reliable.

4. Conclusion

This work introduces the discrete singular convolution (DSC) algorithm for the treatment of plates with mixed and nonuniform boundary conditions. A unified scheme is proposed for treating simply supported, clamped and transversely supported with nonuniform elastic rotational restraint edges. Convergence tests are performed to validate the proposed approach for handling various combinations of the three types of boundary conditions. A number of numerical examples are considered to explore the usefulness and test the accuracy of the present method. The approach has been validated by convergence studies and comparisons with existing results in the literature. It is found that the convergence of the DSC approach is very good and the results agree well with those obtained by other researchers.

We have also computed some new results for plates with combinations of the mixed and nonuniform edges. Frequency parameters for plates with a variety of spring coefficients are predicted. These cases are also validated by convergence tests. All numerical experiments indicate that the proposed DSC approach is a potential method for plate and structural analysis.

Acknowledgements

This work was supported in part by the National University of Singapore. The third author would like to thank Australian Research Council for providing partial financial support through an ARC small grant.

References

[1] Ota T, Hamada M. Fundamental frequencies of simply supported but partially clamped square plates. Bulletin of the Japanese Society of Mechanical Engineering 1963;6:397–403 [in English].
[2] Keer LM, Stahl B. Eigenvalue problems of rectangular plates with mixed boundary conditions. Journal of Applied Mechanics 1972;39:513–20.
[3] Bartlett CC. The vibration and buckling of a circular plate clamped on part of its boundary and simply supported on the remainder. Journal of Mechanical and Applied Mathematics 1963;16:431–40.
[4] Hirano Y, Okazaki K. Vibration of circular plate having partly clamped or partly simply supported edges. Bulletin of the Japanese Society of Mechanical Engineering 1976;19:610–8.

[5] Narita Y. Application of a series-type method to vibration of orthotropic rectangular plates with mixed boundary conditions. Journal of Sound and Vibration 1981;77:345–55.
[6] Fan SC, Chueng YK. Flexural free vibrations of rectangular plates with complex supported conditions. Journal of Sound and Vibration 1984;93:81–94.
[7] Cheung MS. Finite Strip analysis of structures. Ph.D. thesis, University of Calgary, 1971.
[8] Eastep FE, Hemming FG. Natural frequency of circular plates with partially free, partially clamped edges. Journal of Sound and Vibration 1982;84:152–9.
[9] Mizusawa T, Kaijita T. Vibration and buckling of rectangular plates with non-uniform elastic constraints in rotation. International Journal of Solid Structures 1986;23:45–55.
[10] Rao GV, Raju IS, Murthy TVGK. Vibration of rectangular plates with mixed boundary conditions. Journal of Sound and Vibration 1973;30:257–60.
[11] Mizusawa T, Leonard JW. Vibration and buckling of plates with mixed boundary conditions. Engineering Structures 1990;12:285–90.
[12] Chia CY. Nonlinear vibration anisotropic rectangular plates with non-uniform edge constraints. Journal of Sound and Vibration 1985;101:539–50.
[13] Wang X, Bert CW. A new approach in applying differential quadrature to static and free vibration analysis of beams and plates. Journal of Sound and Vibration 1992;162:566–72.
[14] Laura PAA, Gutierrez RH. Analysis of vibrating rectangular plates with nonuniform boundary conditions by using the differential quadrature method. Journal of Sound and Vibration 1994;173:702–6.
[15] Striz AG, Chen W, Bert CW. Static analysis of structures by the quadrature element method (QEM). International Journal of Solid Structures 1994;31:2807–18.
[16] Shu C, Wang CM. Treatment of mixed and nonuniform boundary conditions in GDQ vibration analysis of rectangular plates. Engineering Structures 1999;21:125–34.
[17] Warburton GB. The vibration of rectangular plates. Proceedings of the Institute of Mechanical Engineering 1954;168:371–84.
[18] Leissa AW. The free vibration of rectangular plates. Journal of Sound and Vibration 1973;31:257–93.
[19] Leissa AW, Laura PAA, Gutierrez RH. Vibration of rectangular plates with non-uniform elastic edge supports. Journal of Applied Mechanics 1979;47:891–5.
[20] Liew KM, Wang CM, Xiang Y, Kitipornchai S. Vibration of Mindlin plates. Amsterdam: Elsevier, 1998.
[21] Liew KM, Wang CM. Vibration analysis of plates by the pb2 Rayleigh–Ritz method: mixed boundary conditions, reentrant corners and internal curved supports. Mechanical Structures and Machines 1992;20: 281–92.
[22] Wei GW. Discrete singular convolution for the solution of the Fokker–Planck equations. Journal of Chemical Physics 1999;110:8930–42.
[23] Schwartz L. Théore des distributions. Paris: Hermann, 1951.
[24] Wei GW. Solving quantum eigenvalue problems by discrete singular convolution. Journal of Physics B 2000;33:343–52.
[25] Wei GW. A unified method for solving Maxwell's equation. Proceedings of 1999 Asia-Pacific Microwave Conference Singapore, November 30, 1999. p. 562–5.
[26] Wei GW. A new algorithm for solving some mechanical problems. Computer Methods in Applied Mechanics and Engineering 2001;190:2017–30.
[27] Wan DC, Wei GW. Numerical solutions for unsteady incompressible flow using discrete singular convolution method. International Journal for Numerical Methods in Fluids 2001, submitted for publication.
[28] Wei GW. Generalized Perona–Malik equation for image restoration. IEEE Signal Processing Letters 1999;6:165–8.
[29] Wei GW. Discrete singular convolution method for the Sine-Gordon equation. Physica D 2000;137:247–59.
[30] Ablowitz MJ, Herbst BM, Schober C. On numerical solution of the sine-Gordon equation. Journal of Computational Physics 1996;126:299–314.
[31] Guan S, Lai C-H, Wei GW. Boundary controlled phase separation in a circular domain. Physica D, in press.
[32] Wei GW. A unified method for computational mechanics. In: Wang CM, Lee KH, Ang KK, editors. Computational mechanics for the next millennium. New York: Elsevier, 1999. p. 1049–54.
[33] Wei GW. Vibration analysis by discrete singular convolution. Journal of Sound and Vibration, in press.

[34] Wei GW. Discrete singular convolution for beam analysis. Engineering Structures, in press.
[35] Leissa AW. Vibration of plates (NASA SP 160). Washington DC: US Government Printing Office, 1969.
[36] Qian LW, Wei GW. A note on regularized Shannon's sampling formulae. Journal of Approximation Theory 2001, submitted for publication.
[37] Liew KM, Hung KC, Lam KY. On the use of substructure method for vibration analysis of rectangular plates with discontinuous boundary conditions. Journal of Sound and Vibration 1993;163:451–62.
[38] Nowacki W. Free vibrations and buckling of a rectangular plate with discontinuous boundary conditions. Bulletin de l'Académie Polonaise des Sciences 1955;3:159–67.
[39] Gorman DJ. An exact analytical approach to the free vibration analysis of rectangular plates with mixed boundary conditions. Journal of Sound and Vibration 1984;93:235–47.
[40] Piskunov VH. Determination of the frequencies of the natural oscillations of rectangular plates with mixed boundary conditions. Prikladnaya Mekhanika 1964;10:72–6 [in Ukrainian].
[41] Kurata M, Hamada M. Natural vibrations of partially clamped plates. Proceedings of the American Society of Civil Engineers. Journal of the Engineering Mechanics Division 1963;89:169–86.